following rate constants (using $K = 1.43 \times 10^{10}$ from ref 30)

$$k_{1d} = 150 \pm 12\ M^{-1}\ s^{-1}$$

$$k_{2d} = 300 \pm 20\ M^{-1}\ s^{-1}$$

$$k_{3d} = (3.4 \pm 0.2) \times 10^{4}\ M^{-1}\ s^{-1}$$

These values cannot be directly compared with the results of Sutter et al.,[31] which refer to strongly acidic solutions.

The hypomanganate ion, MnO_4^{3-}, detected by DARSS as an intermediate is not stable enough in moderately alkaline solutions. Its likely fate is disproportionation yielding manganate(VI) and the product manganese(IV), eq 13. The yellow product solutions

$$2MnO_4^{3-} \xrightarrow{fast} MnO_4^{2-} + Mn(IV)_{(sol)} \quad (13)$$

$$Mn(IV)_{(sol)} \xrightarrow{slow} MnO_2 \quad (14)$$

contain an unknown, soluble form of manganese(IV), observed previously in various oxidations by permanganate ion.[6-8] It can also be prepared by dissolving freshly precipitated MnO_2 in phosphoric acid and reveals oxidizing properties distinct from those of manganese(III).[32] Although the yellow species may be colloidal MnO_2 in some instances, evidence is accumulating in support of bridged dinuclear phosphatomanganese(IV)[32-34] or sulfatomanganese(IV)[35] species, at least in strongly acidic solutions. The existence of manganese(IV) complexes with polyhydroxy compounds in alkaline media is well established.[36]

The yellow species in this work is gradually converted to insoluble MnO_2, the rate of precipitation depending on the pH, electrolyte concentration, etc. The MnO_4^{2-} formed in eq 13 disproportionates according to eq 11. The permanganate ion produced in eq 11 is consumed for sulfite oxidation as depicted by eq 6-10.

The mechanistic conclusions emerging from the present study are also relevant to the nature and behavior of intermediates in the permanganate oxidation of olefinic and acetylenic substrates. In these cases, manganese(V) esters are routinely invoked as short-lived intermediates, but the unambiguous detection of these species remains the subject of further work. The lifetimes of the hypothetic manganate(V) esters may be too short for detection especially in less alkaline or acidic media. The occurrence of soluble manganese(IV) intermediates is, however, a distinct possibility in acidic solutions.

Acknowledgment. This work was partially supported by the R. A. Welch Foundation and the National Science Foundation. L.I.S. thanks the University of Texas at Arlington for a Visiting Professorship in the spring semester of 1983.

Registry No. MnO_4^-, 14333-13-2; SO_3^{2-}, 14265-45-3.

(31) Sutter, J. H.; Colquitt, K.; Sutter, J. R. *Inorg. Chem.* **1974**, *13*, 1444.
(32) Jáky, M.; Shafirovich, V. Ya.; Simándi, L. I. *Inorg. Chim. Acta* **1984**, *90*, L39.
(33) Jáky, M.; Simándi, L. I., unpublished results.
(34) Cooper, S. R.; Calvin, M. *J. Am. Chem. Soc.* **1977**, *99*, 6623.
(35) Luneva, N. P. Abstracts of 4th International Symposium on Homogeneous Catalysis, Sept 24-28, 1984, Leningrad, USSR, Book IV, p 182. Luneva, N. P.; Shafirovich, V. Ya.; Shilov, A. E. *Kinet. Katal.* **1984**, *25*, 1252.
(36) Magers, K. D.; Smith, C. G.; Sawyer, D. T. *Inorg. Chem.* **1978**, *17*, 515.

Mechanism of Hydrolysis of 2-*tert*-Butyl-2-methoxy-1,3-dithiolane. Rate-Determining Deprotonation in the Breakdown of Tetrahedral Intermediate

Tadashi Okuyama* and Takayuki Fueno

Contribution from the Faculty of Engineering Science, Osaka University, Toyonaka, Osaka 560, Japan. *Received September 13, 1984. Revised Manuscript Received February 16, 1985*

Abstract: Hydrolysis of 2-*tert*-butyl-2-methoxy-1,3-dithiolane (**1b**), as well as 2-methoxy-1,3-dithiolane (**1a**), proceeds through a three-stage process to lead to an (*S*)-2-mercaptoethyl thiocarboxylate (**4**), which involves 1,3-dithiolan-2-ylium ion (**2**) and 2-hydroxy-1,3-dithiolane (**3**) as intermediates. The initial expulsion of methanol catalyzed by acid (**1** → **2**) is rate determining at higher pHs, but the decay of **3**, which is catalyzed both by acid and base, becomes the slow step at low pHs. When the isolated salt of 2-*tert*-butyl-1,3-dithiolan-2-ylium ion (**2b**) was used, kinetic behavior of the base-catalyzed decay of **3b** was examined in detail. This reaction involves deprotonation of the neutral **3b** as a rate-determining step at high pHs but the breakdown of the anionic **3b**$^-$ becomes rate determining with increasing hydronium ion or buffer concentration.

Our recent investigations showed that ketene dithioacetals undergo acid-catalyzed hydrolysis through partially reversible protonation of the carbon-carbon double bond (eq 1).[1-5] De-

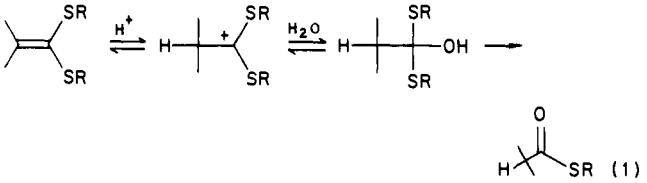

(1)

protonation of the β-hydrogen is competitive with hydration of the intermediate dithio carbocation. This was ascribed to the very slow rate of hydration of the dithio carbocation.[6] For the same reason, the dithio cations are stable and can be isolated as salts. In some cases, the equilibrium constants for the hydration could

(1) Okuyama, T.; Fueno, T. *J. Am. Chem. Soc.* **1980**, *102*, 6590-6591; **1983**, *105*, 4390-4395.
(2) Okuyama, T.; Kawao, S.; Fueno, T. *J. Am. Chem. Soc.* **1983**, *105*, 3320-3326.
(3) Okuyama, T.; Kawao, S.; Fujiwara, W.; Fueno, T. *J. Org. Chem.* **1984**, *49*, 89-93.
(4) Okuyama, T.; Kawao, S.; Fueno, T. *J. Org. Chem.* **1984**, *49*, 85-88.
(5) Okuyama, T. *J. Am. Chem. Soc.* **1984**, *106*, 7134-7139.
(6) Okuyama, T.; Fujiwara, W.; Fueno, T. *J. Am. Chem. Soc.* **1984**, *106*, 657-662.

0002-7863/85/1507-4224$01.50/0

be determined directly by a spectrophotometric method.[5,6] The exact kinetic analysis of breakdown of the tetrahedral intermediate is then possible. Such an analysis was carried out before for the reactions involving the 2-methyl-1,3-dithiolan-2-ylium ion.[5] In order to extend this analysis, we have prepared unsubstituted 2-methoxy-1,3-dithiolane and the 2-*tert*-butyl derivative (**1a** and **1b**) as precursors of the cations **2** which have no β-hydrogen capable of deprotonation. It was found that base-catalyzed decay

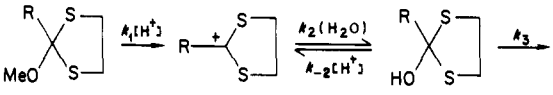

1a, R = H
1b, R = *t*-Bu

2 3

4

of the tetrahedral intermediate **3b** involves proton transfer from the hydroxyl group of **3b** to the catalyst base as a rate-determining step. This reaction was characterized by the pH-rate correlation, buffer catalysis, and kinetic isotope effects. A similar observation of rate-limiting deprotonation of a tetrahedral intermediate of the oxygen analogue has recently been published.[7] Our results on the reactions of eq 2 are presented herein.

Results

Preparation of Substrates. The perchlorate salt of 2-*tert*-butyl-1,3-dithiolan-2-ylium ion (**2b**) was obtained from the reaction of trimethylacetyl chloride with 1,2-ethanedithiol in the presence of perchloric acid and isolated as yellow crystallines by treatments with acetic anhydride and dry ether. Reaction of the salt with methanol in the presence of base afforded 2-*tert*-butyl-2-methoxy-1,3-dithiolane (**1b**) (eq 3).

$$Me_3CCOCl + HS(CH_2)_2SH + HClO_4 \rightarrow \mathbf{2b}\cdot ClO_4^- \xrightarrow{MeOH} \mathbf{1b} \quad (3)$$

Reaction of formic acid with ethanedithiol in the presence of perchloric acid resulted in the formation of a waxy solid instead of the carbocation salt. The solid material was identified as 1,2-bis(1,3-dithiolan-2-ylthio)ethane (**5**), which was also obtained by the reaction of trimethoxymethane with ethanedithiol,[8] and was converted to dithiolanylium (**2a**) perchlorate by the treatments with $HClO_4$ in acetic anhydride (eq 4). The salt **2a** was then

$$HCO_2H \text{ (or } HC(OMe)_3) + HS(CH_2)_2SH \xrightarrow{H^+}$$

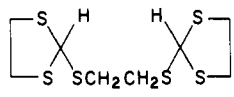

$$\xrightarrow[Ac_2O]{HClO_4} \mathbf{2a}\cdot ClO_4^- \xrightarrow{MeOH} \mathbf{1a} \quad (4)$$

5

converted to the 2-methoxy derivative **1a**. Similar treatments of 2-methyl-1,3-dithiolan-2-ylium salts[9] with methanol resulted in the deprotonated derivative 2-methylene-1,3-dithiolane.

Hydrolysis. Hydrolysis of 2-methoxy-1,3-dithiolanes **1a** and **1b** takes place in acid solutions with formation of thio esters **4a** and **4b** which absorb UV light at 233 nm. Rates of the hydrolysis were spectrophotometrically measured by following usually the formation of **4** (233 nm) in aqueous solutions (containing 1% acetonitrile) at 25 °C. The ionic strength was maintained at 0.50 M with KCl except for concentrated acids. Pseudo-first-order plots were usually linear down to 90% conversion. Rate constants k_{obsd} obtained in HCl and $HClO_4$ solutions are given in Table S1 (supplementary material). Rates of hydrolysis of **1b** were also measured in formate and acetate buffer solutions and were found to be independent of buffer concentrations within experimental uncertainties (Table S2).

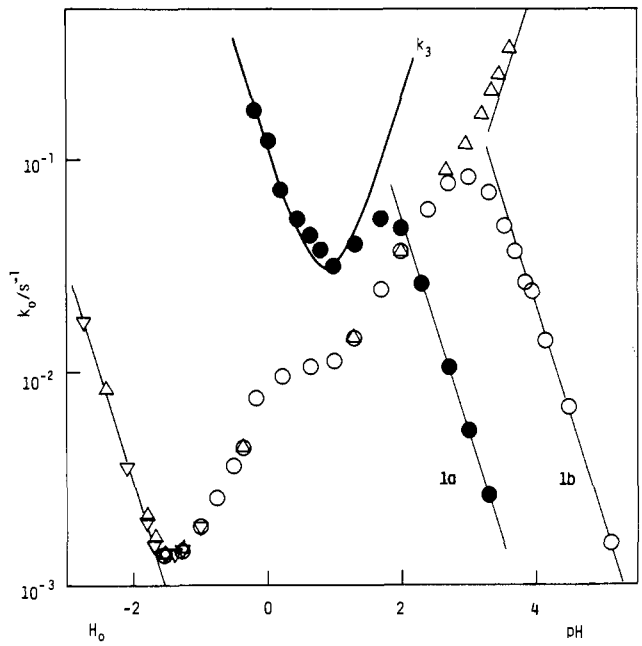

Figure 1. Acidity–rate correlations for the hydrolyses of **1a** (●) and **1b** (○). Rate constants for the decay of **2b** (△) and the formation of **2b** from **4b** (▽) are also shown.

The rate constants k_{obsd} are shown plotted logarithmically against the pH or H_0 acidity function[10] in Figure 1. The acidity–rate profiles for **1a** and **1b** are apparently complicated and quite different from each other. In the pH regions (pH 1.3–2 for **1a** and pH 2.7–3.3 for **1b**) where the profiles show maximum, the induction period was observed and k_{obsd} was determined from the latter part of the first-order plot.

Carbocation Intermediates. The absorption of the intermediate carbocation **2b** could be observed (λ_{max} 331 nm) at [HCl] >0.01 M during the hydrolysis of **1b**: the appearance of absorbance at 331 nm is instantaneous and the rate of the disappearance, which follows pseudo-first-order kinetics, is identical with that of the formation of the thiol ester product **4b** as monitored at 233 nm (Table S1). The absorbance at 330 nm immediately after addition of **1b** in acid was obtained by extrapolating the decreasing absorbance to the zero time by means of the conventional UV method. The results are summarized in Table S3. The plot of the absorbances against pH (H_R[10] at higher acidities) fits well a sigmoid curve of $pK_R = 1.16 \pm 0.04$ as shown in Figure 2.

In strong acid, the initial absorbance at 330 nm (which developed instantaneously) was that expected for **2b** at the initial concentration of **1b**. The absorbance decreased with isosbestic points at about 250 and 225 nm and simultaneous formation of the absorption of **4b**. The ultimate absorption is that of a mixture of **2b** and **4b**, and the absorbance at 330 nm increases with acidity. The same results were obtained by starting with the isolated salt of **2b** as summarized in Table S4. A plot of the absorbances against H_R follows a sigmoid curve of $pK_R = -3.32 \pm 0.04$ (Figure 2). The reverse absorbance changes were observed by starting with **4b**. The ultimate absorbances agreed with those obtained by starting with **1b** (Table S4 and Figure 2). The rate constants for the appearance of **2b** (330 nm) from **4b** were also determined (Table S4) and are plotted with inverted triangles in Figure 1.

The absorption of the unsubstituted cation **2a** (λ_{max} 333 nm) could be observed only in very strong acid ([$HClO_4$] > 3.5 M) during the hydrolysis of **1a**. The absorption developed very rapidly and decreased gradually. This decrease in absorbance at 333 nm accompanied the decrease in the 233-nm absorbance due to the thiol ester product **4a**. The initial absorbances at 333 nm obtained

(7) McClelland, R. A. *J. Am. Chem. Soc.* **1984**, *106*, 7579–7583.
(8) Hurtley, W. R. H.; Smiles, S. *J. Chem. Soc.* **1926**, 2263–2270.
(9) Okuyama, T. *Tetrahedron Lett.* **1982**, *23*, 2665–2666.
(10) Kresge, A. J.; Chen, H. J.; Capen, G. L.; Powell, M. F. *Can. J. Chem.* **1983**, *61*, 249–256.

Table I. Buffer Effects on the Rate of Formation of **4b** from **2b**

buffer (pK_a)[a]	pH	$10^2\Delta k_{max}$, s^{-1} [b]	10^2K_{app}, M[b]	k_i, M^{-1} s^{-1} [c]	$k_B\alpha$, M^{-1} s^{-1}	k_B, M^{-1} s^{-1}
cyanoacetate (2.43)	2.33	10.5 (0.3)	15.6 (3.4)	0.27	0.46	0.92
	2.78			0.28	0.37	0.50
chloroacetate (2.86)	2.64	26.3 (1.1)	38.3 (4.1)	0.46	0.64	1.28
	2.64			0.33	0.46	0.92
	3.06			0.79	0.96	1.32
methoxyacetate (3.53)	2.80			0.64	0.84	4.2
	2.95	62.4 (3.1)	49.4 (5.6)	1.01	1.26	5.04
	3.14			1.25	1.49	4.47
formate (3.77)	3.10			1.78	2.14	10.7
	3.29			3.49	4.07	14.5

[a] Taken from: Sober, H. A., Ed. "CRC Handbook of Biochemistry"; CRC Press: Cleveland, OH, 1968. [b] Standard deviations are given in parentheses. [c] Obtained as $\Delta k_{max}/K_{app}$ or an initial slope.

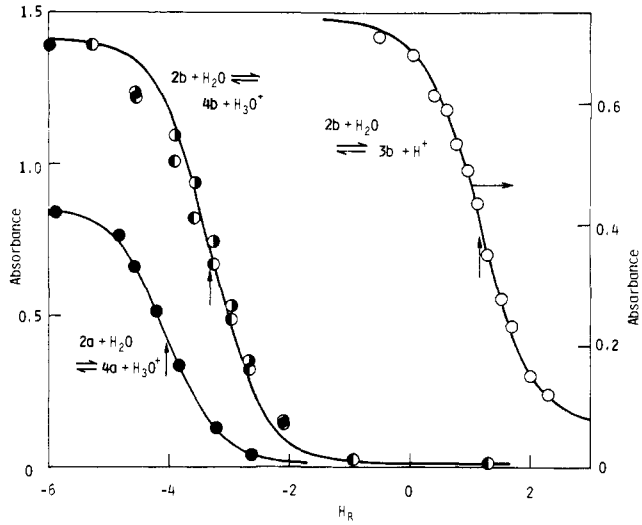

Figure 2. Acidity dependences of equilibrium absorbances: (●) initial absorbance at 333 nm starting with **1a** (1.08×10^{-5} M); (○) initial absorbance at 330 nm starting with **1b** (0.90×10^{-5} M) (right ordinate). (◐ and ◑) ultimate absorbances at 330 nm starting with **2b** (1.75×10^{-5} M) and **4b** (data obtained at 0.85×10^{-5} M are corrected for 1.75×10^{-5} M), respectively.

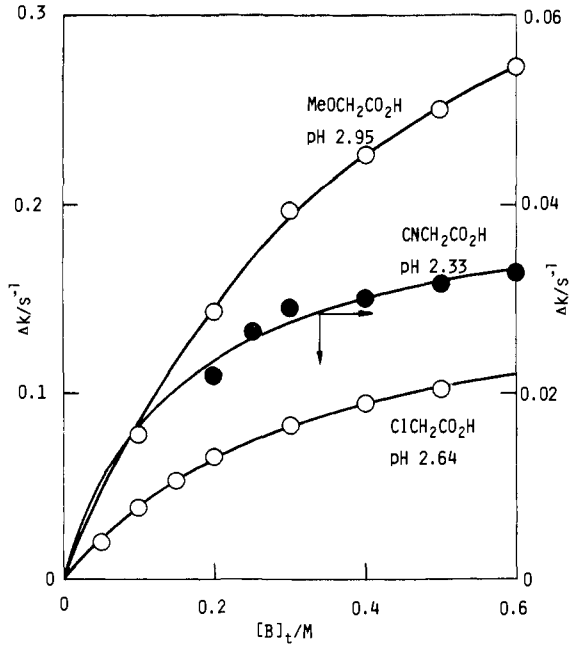

Figure 3. Buffer dependences of rate constants for the decay of **2b** in carboxylate buffer solutions indicated.

by the extrapolation are given in Table S3 and are plotted against H_R in Figure 2 to give a sigmoid curve of $pK_R = -4.04 \pm 0.02$.

Kinetic behavior (observable by conventional UV method) of the reaction of the preformed (isolated) cation **2b** was also examined and found to be essentially the same as that of **1b** below pH 2. At higher pHs, however, the (slow) rate of appearance of **4b**, which follows the instantaneous disappearance of **2b**, increases with increasing pH as shown with triangles in Figure 1. Data are given in Table S5.

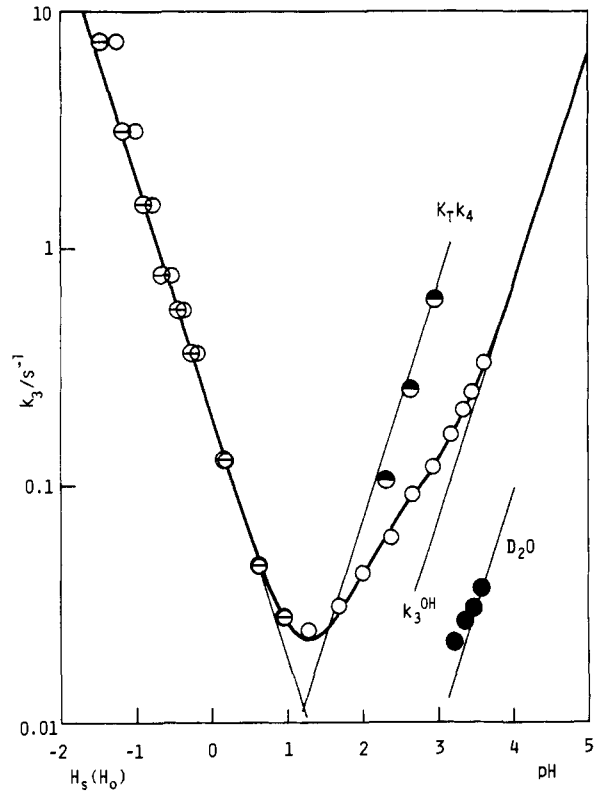

Figure 4. Acidity–k_3 profile for the decay of **3b**. The k_3 values are plotted against either the H_0 (pH) (○) or H_S (⊖) acidity function. The solid curve was calculated by eq 12 by using parameters given in Table II. The observed rate constants (●) for the decay of **2b** in D_2O and k_{max} (◓) obtained from the buffer dependences are also shown.

This reaction was strongly buffer-catalyzed, but the buffer effects were found to level off with increasing concentration of the buffer $[B]_t$ as shown in Figure 3 (data given in Table S7). The saturation curve seems to follow eq 5 where Δk ($=k_{obsd} - k_0$)

$$\Delta k = \Delta k_{max}[B]_t/(K_{app} + [B]_t) \quad (5)$$

is a rate increase induced by the buffer at total concentration $[B]_t$. Theoretical curves in Figure 3 are calculated by eq 5 with parameters given in Table I, which were obtained by a nonlinear least-squares treatment of the data by using a calculated value for k_0 (by eq 10 given below). In all other cases, the initial slopes of the k_{obsd}–$[B]_t$ plots at low concentrations of the buffer were obtained and are given as k_i in Table I. The calculated k_0 (eq 10) was used here again to obtain the initial slope k_i. The slope k_i is correlated with the parameters of eq 5 according to eq 6.

$$k_i = \Delta k_{max}/K_{app} \quad (6)$$

Rates of appearance of **4b** starting with **2b** were also measured in dilute DCl solutions at [DCl] = (1–5) × 10^{-4} M. Because of the added cation salt **2b**, pD measured was somewhat lower than –log [DCl]. Observed rate constants k_{obsd} were nearly $^1/_8$ of those obtained in H_2O at the same pH. Data are given in Table S5 and plotted with closed circles in Figure 4.

Reaction of the preformed cation **2a** did not give reproducible kinetics as monitored at 233 nm. This may probably be due to some mixing problems; reactions of **2a** with water are extremely rapid (>100 s^{-1}). The disappearance of **2a** was too rapid to determine the rate by the stopped-flow method. The rates of disappearance of **2b** could be measured in very dilute HCl solutions. The average of k_{obsd} was 9.4 s^{-1} in 1:1 (v/v) CH_3CN–H_2O at the ionic strength of 0.25 M.

Discussion

The kinetic behavior of hydrolysis of **1** may be accommodated by the three-stage reaction process of eq 2, which is similar to that of hydrolysis of ortho esters.[11-13] The high-pH portions of the pH-rate profiles in Figure 1, where the rates increase with decreasing pH with a slope of –1, must reflect the acid-catalyzed expulsion of methanol from **1**; the first step is rate-determining at pH >2 for **1a** (k_1 = 5.28 M^{-1} s^{-1} and at pH >3.5 for **1b** (k_1 = 202 M^{-1} s^{-1}).

The rate-determining step switches to the third step (eq 2) at pH 2–3 as the pH is lowered. Disappearance of the absorption of the cation **2b** was instantaneous, but appearance of the thiol ester product **4b** was slow in the pH region 2–4 when the reaction was started with the preformed cation **2b**. Below pH 2, the reaction was apparently biphasic. The instantaneous reaction of **2b** does not go to completion but leaves some absorption of **2b**, which slowly disappears. The rate of the latter reaction, monitored at 330 nm, agrees with that of the appearance of the thiol ester **4b** (233 nm). This change is accompanied by isosbestic points and must correspond to the third step. The former rapid reaction must be the equilibrium formation of **3b**. The initial absorbance at 330 nm obtained by the extrapolation on a conventional UV spectrophotometer must correspond to the concentration of **2b** in equilibrium with **3b**. The same spectral behavior was observed by starting with **1b** in acid solutions. The midpoint of the sigmoid curve (Figure 2) therefore refers to pK_2 of the equilibrium **2** ⇌ **3**.

The rate of hydrolysis of **1b** decreases with increasing acidity below pH 3 with two plateau regions at pH 0–1 and below H_0 –1 (Figure 1). The decrease must primarily reflect the decrease in the equilibrium concentration of **3b**. The observed rate constant k_{obsd} must be described by eq 7. When the K_2 value obtained

$$k_{obsd} = K_2 k_3/(K_2 + h_R) \quad (7)$$

above is used, k_3 can be calculated and are shown plotted against H_0 (pH) in Figure 4. Above pH 2.5, k_{obsd} was obtained by starting with **2b**. The profile obtained shows both acid and base catalyses but deviates from that expected for simple acid- and base-catalyzed reactions: upward deviations (a steep slope) at H_0 <0 and a gradual slope (<1) of the base-catalyzed portion above pH 2.

The steep increase in acid-catalyzed rate must reflect the steep dependence of the sulfur protonation on acid concentration[14-16] and can be accommodated by a modified acidity function H_S defined by eq 8 for the sulfur protonation (barred circles in Figure

$$H_S = 1.3H_0 - 0.3(\log [H^+]) \quad (8)$$

Scheme I

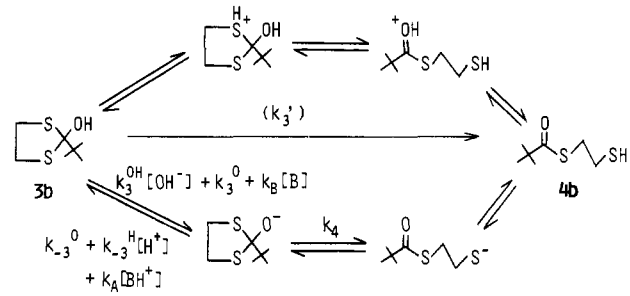

Table II. Kinetic Parameters for the Hydrolysis of

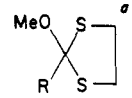

	1a (R = H)	**1b** (R = *t*-Bu)	**1c** (R = Me)[b]
k_1, M^{-1} s^{-1}	5.28	202	(49)
k_2, s^{-1}		11.2	21
k_{-2}, M^{-1} s^{-1}	4.2	162	39
pK_2		1.16 ± 0.04	0.27
k_3^{OH}, M^{-1} s^{-1}		7.0 × 10^9	
k_3^0, s^{-1}		0.091	
$K_T k_4$, M s^{-1}	2 × 10^{-3}	7.0 × 10^{-4}	1.4 × 10^{-3}
k_{-3}^0/k_4		0.10	
(k_{-3}^H/k_4), M^{-1}		130	
k_3^a, M^{-1} s^{-1}	0.11	0.20	0.28
k_{-3}, M^{-1} s^{-1}		3.4 × 10^{-5}	9 × 10^{-5}
pK_R[c]	–4.04 ± 0.02	–3.32 ± 0.04	–4.6

[a] 25 °C, ionic strength 0.50 M. [b] Taken from ref 5. [c] For the equilibrium **2** ⇌ **4**.

4). Similar dependence of the rate on acidity was observed for the acid-catalyzed decay of 2-hydroxy-2-methyl-1,3-dithiolane (**3c**) during the hydrolysis of 2-methylene-1,3-dithiolane.[5] The observed complication of the H_0–k_0 profile is due to the different dependences of k_3 and K_2 on the acidities (H_S vs. H_R).

The base-catalyzed decay of **3b** involves another changeover of the rate-determining step. The rate is strongly buffer-dependent, but the rate increase levels off at higher concentrations of the buffer. The rate-determining step must change from a buffer-dependent to buffer-independent one as $[B]_t$ increases. The maximum rate constants induced by added buffer were obtained by the curve fittings according to eq 5 (Figure 3) and are plotted with half-filled circles in Figure 4. These points fall closely on a line of slope 1.0, defined by the rate constant $K_T k_4$ = 7.0 × 10^{-4} M s^{-1}, where K_T is the dissociation constant of **3b** ($K_T = k_3^0/k_{-3}^H = k_3^{OH}K_w/k_{-3}^0$). On the other hand, the rate constants k_3 approach a line of slope 1.0, defined by $k_3^{OH}K_w$ = 7.0 × 10^{-5} M s^{-1}, at high pH.

These results are consistent with the reaction mechanism of Scheme I which involves dissociation of **3b**. The rate constant k_3 can be described by eq 9 according to Scheme I. At high pH

$$k_3 = \frac{(k_3^{OH}K_w/[H^+] + k_3^0 + k_B[B])k_4}{k_{-3}^0 + k_{-3}^H[H^+] + k_A[BH^+] + k_4} + k_3^a h_S \quad (9)$$

and limiting zero buffer concentration, diffusion-controlled proton transfer from **3b** to OH^- (k_3^{OH}) is mostly rate determining. Hydronium ion and general acids accelerate the reverse of this step, and the rate ("k_{-3}") eventually exceeds the rate of unimolecular decay of the anionic intermediate (k_4) at higher concentrations of the acids: the latter step becomes rate determining. At limiting zero buffer concentration, eq 9 is simplified to eq 10. The theoretical curve of Figure 4 is calculated by eq 10 with rate constants summarized in Table II. The value of k_3^{OH} (7 × 10^9 M^{-1} s^{-1}) is reasonable for the diffusion-controlled reaction involving

$$k_3 = \frac{k_3^{OH}K_w/[H^+] + k_3^0}{k_{-3}^0/k_4 + k_{-3}^H[H^+]/k_4 + 1} + k_3^a h_S \quad (10)$$

(11) Cordes, E. H.; Bull, H. G. *Chem. Rev.* **1974**, *74*, 581–603.
(12) (a) Ahmad, M.; Bergstrom, R. G.; Cashen, M. J.; Kresge, A. J.; McClelland, R. A.; Powell, M. F. *J. Am. Chem. Soc.* **1977**, *99*, 4827–4829. (b) Ahmad, M.; Bergstrom, R. G.; Cashen, M. J.; Chiang, Y.; Kresge, A. J.; McClelland, R. A.; Powell, M. F. *Ibid.* **1979**, *101*, 2669–2677.
(13) Chiang, Y.; Kresge, A. J.; Lahti, M. O.; Weeks, D. P. *J. Am. Chem. Soc.* **1983**, *105*, 6852–6855 and references cited therein.
(14) Bonvicini, P.; Levi, A.; Lucchini, V.; Scorrano, G. *J. Chem. Soc. Perkin Trans. 2* **1972**, 2267–2269.
(15) Bonvicini, P.; Levi, A.; Lucchini, V.; Modena, G.; Scorrano, G. *J. Am. Chem. Soc.* **1973**, *95*, 5960–5964.
(16) Perdoncin, G.; Scorrano, G. *J. Am. Chem. Soc.* **1977**, *99*, 6983–6986.

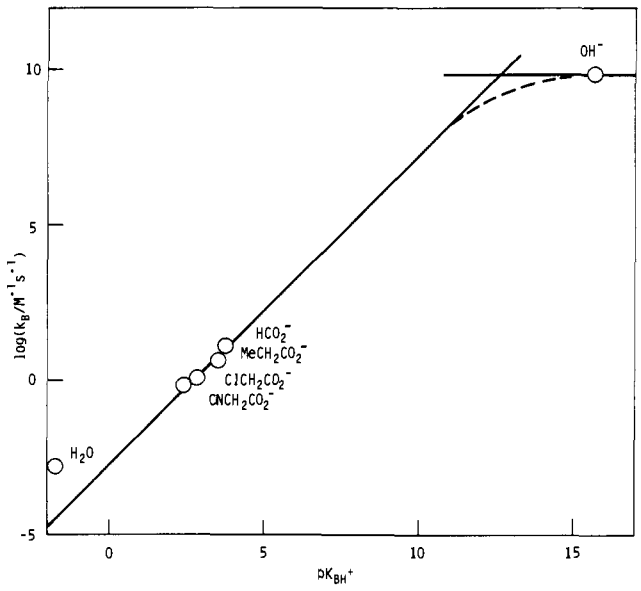

Figure 5. Brønsted plot for the base-catalyzed decay of **3b**.

OH^-.[17] The deprotonation and ring-opening process contribute equally to the overall k_3 at pH 2.16.

From eq 5,[18] 9, and 10, the parameters k_{max} and K_{app} are described by eq 11 and 12, respectively, where α stands for the base fraction of the buffer. The initial slope k_i of the buffer

$$k_{max} = k_B k_4 \alpha / k_A(1 - \alpha) = K_T k_4 / [H^+] \quad (11)$$

$$K_{app} = (k_{-3}^{O} + k_{-3}^{H}[H^+] + k_4)/k_A(1 - \alpha) \quad (12)$$

$$k_i = k_B/(k_{-3}^{O}/k_4 + k_{-3}^{H}[H^+]/k_4 + 1) \quad (13)$$

dependence, which is equal to $\Delta k_{max}/K_{app}$, can be described by eq 13. The catalytic constants k_B for the deprotonation of **3b** were calculated by eq 13 and are given in Table I.

The catalytic constants k_B calculated seem to involve some experimental uncertainties, but the averages are plotted against pK_a of the conjugate acid of the catalysts in Figure 5. Four points for carboxylates seem to fall on a line of slope $\beta = 1.0$. The line crosses a horizontal line of the diffusion-controlled limit of k_3^{OH} at $pK_a = 12.6$. This correlation conforms to the "Eigen curve"[17] for a simple proton transfer between two heteroatoms, and the pK_a value of the crossing point must correspond to pK_T of the intermediate **3b**. This pK_T is not far from the estimated value (13.3) for **3b** based on the structure–reactivity correlations.[19,20]

When the pK_T (12.6) obtained from the Eigen curve and the constants listed in Table II are used, the following rate constants can also be calculated: $k_{-3}^{O} = 2.8 \times 10^8\ s^{-1}$, $k_{-3}^{H} = 3.6 \times 10^{11}\ M^{-1}\ s^{-1}$, and $k_4 = 2.8 \times 10^9\ s^{-1}$. The value of k_{-3}^{H} seems to be somewhat too large, exceeding the diffusion limit. The water reaction of **3b** may involve direct formation of **4b** (k_3'), but such considerations do not improve much fits of the curve. The excess value of k_{-3}^{H} may have arisen from the accumulation of errors in evaluation of kinetic parameters. There is another problem that should be mentioned here. The rate constants $k_{-2}[H^+]$ and k_3 are equal to each other around pH 3, and above this pH, k_3 exceeds $k_{-2}[H^+]$; that is, the hydration of **2b** (k_2 process) becomes the rate-determining step of the decay of **2b**. Nevertheless, the k_{obsd} obtained from the formation of **4b** is essentially equal to k_3 since k_2 is much greater than $k_{-2}[H^+]$ and k_3.

McClelland recently found curved buffer dependences of the rate of base-catalyzed breakdown of 2-hydroxy-2-phenyl-1,3-dioxolane and concluded that the reaction involves rate-determining deprotonation.[7] In this case, the change in the rate-determining step of the base-catalyzed reaction was observed by increasing buffer concentration but not by changing only the pH of the medium.[12,21] Buffer catalysis was observed of the breakdown of the anionic dioxolane intermediate in contrast to the dithiolane case. The thiolate product 4^- is more easily formed than the alkoxide product **6**.

$$\underset{\mathbf{4}^-}{RCOSCH_2CH_2S^-} \qquad \underset{\mathbf{6}}{PhCOOCH_2CH_2O^-}$$

Another example of closely related reactions examined in detail is the addition of thiolate anions to acetaldehyde.[22] Mechanisms of the catalysis are delicately dependent on the basicity of the thiolate anion. The addition of the anion of methyl mercaptoacetate to acetaldehyde was found to involve proton transfer as a kinetically significant step, and the mechanism presented for this reaction is the microscopic reverse of the process given in Scheme I. The rate-determining step of the base-catalyzed reaction changes with changing pH and buffer concentration. This occurs because k_{-3}^{O} and k_4 are comparable in their magnitude: $k_{-3}^{O} \simeq k_4 \simeq 4 \times 10^7\ s^{-1}$ for $^-SCH_2CO_2Me + MeCHO$. The value of k_{-3}^{O} depends on the dissociation constant K_T ($=k_3^{OH}K_w/k_{-3}^{O}$) since k_3^{OH} is the diffusion-controlled proton transfer from **3** to OH^- and independent of the structure of **3** ($0.6–1 \times 10^{10}\ M^{-1}\ s^{-1}$).[22] Moreover, K_T and thus k_{-3}^{O} are rather insensitive to the basicity of the thiolate, but k_4 decreases with increasing basicity of the thiolate. The k_4 step is always rate determining in the case of basic thiolate + acetaldehyde. In the present case, k_4 is greater than that found for $-SCH_2CO_2Me$ ($pK_a = 7.83$) + MeCHO in spite of the higher basicity of $^-SCH_2CH_2SH$ ($pK_a = 10.75$). The cyclic structure of **3b** may also be a factor to reduce the rate of the C–S bond cleavage.[23] The large k_4 value observed for the present reaction may be ascribed to the stabilization of the transition state by the thiol ester conjugation as compared with the case of acetaldehyde.

Solvent isotope effects on the rate of reaction of **2b** were examined near pD 3.5. The observed rate constants in this pH region should be close to k_3. The k_3 is about 8-fold greater in H_2O than in D_2O at the same pH(D). Proton transfer from the hydroxyl group of **3b** to hydroxide ion is concluded to be mostly rate determining in this pH region. Primary kinetic isotope effects on the proton transfer between heteroatoms are greatly dependent on the difference in pK_a of the proton donor and that of the conjugate acid of the proton acceptor, and the difference of about 3 pK units in the present case may result in the very small primary isotope effects.[24,25] The rates are compared here at the same oxonium ion concentration $[H^+(D^+)]$. However, since the ionization constant of D_2O is smaller than that of H_2O by a factor of 7.1–7.4,[26–29] concentration of OD^- in D_2O is smaller than that of OH^- in H_2O by this factor at the same pH(D). Isotope effects observed must come mostly from this difference in concentrations of the base in the two media.

When the acidity of the medium becomes still higher, the rate of slow disappearance of **2b** increases again. Moreover, the ultimate absorbance remains to some extent. This occurs because the reverse of the third step (**4** → **3**) is appreciable in this acidity range. The rate constant observed must be the sum of the forward and reverse reactions. The formation of **2b** was in fact observed

(17) Eigen, M. *Angew. Chem., Int. Ed. Engl.* **1964**, *3*, 1–72.
(18) In eq 5, k_{obsd} is essentially equal to k_3 in the pH range of the buffers used.
(19) Fox, J. P.; Jencks, W. P. *J. Am. Chem. Soc.* **1974**, *96*, 1436–1449.
(20) Sayer, J. M.; Jencks, W. P. *J. Am. Chem. Soc.* **1976**, *98*, 7777–7789.
(21) McClelland, R. A.; Ahmad, M. *J. Org. Chem.* **1979**, *44*, 1855–1860.
(22) Gilbert, H. F.; Jencks, W. P. *J. Am. Chem. Soc.* **1977**, *99*, 7931–7947. Jencks, W. P. *Acc. Chem. Res.* **1976**, *9*, 425–432; **1980**, *13*, 161–169.
(23) McClelland, R. A.; Seaman, N. E. *Can. J. Chem.* **1984**, *62*, 1608–1612.
(24) Bergman, N.-A.; Chiang, Y.; Kresge, A. J. *J. Am. Chem. Soc.* **1978**, *100*, 5954–5956.
(25) Cox, M. M.; Jencks, W. P. *J. Am. Chem. Soc.* **1978**, *100*, 5956–5957.
(26) Covington, A. K.; Robinson, R. A.; Bates, R. G. *J. Phys. Chem.* **1966**, *70*, 3820–3824.
(27) Pentz, L.; Thornton, E. R. *J. Am. Chem. Soc.* **1967**, *89*, 6931–6938.
(28) Gold, V.; Lowe, B. M. *J. Chem. Soc. A* **1967**, 936–943.
(29) Goldblatt, M.; Jones, W. M. *J. Chem. Phys.* **1969**, *51*, 1881–1894.

by starting with **4b**, and the k_{obsd} obtained from appearance of **2b** are identical with those obtained from the reaction of **2b** or **1b** (disappearance of **2b**). From the ultimate absorbance at 330 nm, pK_R for the equilibrium **2b** ⇌ **4b** was determined (−3.32).

The acidity–rate profile for the hydrolysis of **1a** below pH 1.5 is a part of an inverse bell-type for the acid- and base-catalyzed decay of hydrogen ortho thio ester **3a**. Both the first and second steps (eq 2) are rapid, and the equilibrium is in favor of formation of **3a** in the acidity range −0.5–1.5. The equilibrium constant K_2 is large, and k_{obsd} is nearly equal to the rate constant k_3 for the third step as is obvious from eq 9. Rate constants for the acid- and base-catalyzed decay of **3a** are $k_3^a = 0.11\ M^{-1}\ s^{-1}$ and $K_T k_4 = 2 \times 10^{-3}\ M\ s^{-1}$, respectively (Figure 1). Here, the base-catalyzed reaction is ascribed to the rate-determining decay of the anionic intermediate **3a**$^-$. If we use an estimated value for K_T (pK_T = 12), k_4 is calculated to be $2 \times 10^9\ s^{-1}$, which is close to that for **3b**.

The absorbance of the cation **2a** (333 nm) was observable only in very strong acid ([$HClO_4$] > 3.5 M or H_0 <−1.5). The absorbance decreases very slowly, and this change accompanies the decay of the thiol ester **4a**. The initial absorbances at 333 nm follow a sigmoid curve of $pK_R = -4.04 \pm 0.02$ when plotted against H_R. These observations are rationalized as follows. All the reactions involved in the three-stage process of eq 2 are rapid, and the main species present in this acidity range are **2a** and **4a** in equilibrium. The slow decrease in absorption may be due to the hydrolysis of **4a** to give 1,2-ethanedithiol and formic acid (eq 14).

$$\mathbf{2a} \rightleftharpoons \mathbf{4a} \rightarrow HCO_2H + HS(CH_2)_2SH \qquad (14)$$

Similar hydrolysis of the thiol ester **4** of higher carboxylic acids were negligible under the acidities used.

All the rate constants of elementary processes are summarized in Table II for **1a** and **1b** together with those for the 2-methyl derivative **1c**[5] for the sake of comparison. The reactions **1** → **2** and **3** → **2** closely resemble each other, and k_{-2} is estimated to be $0.8k_1$.[30] Either of k_1 or k_{-2} can then be evaluated from the other. These reactions were found to be nearly independent of buffer. This means that general base catalysis of the reverse hydration of the carbocations **2** is negligibly small. This is in contrast to the occurrence of general catalysis of hydration of more stable carbocations.[6]

Both k_1 and k_{-2} increase with increasing bulk of the 2 substituent (H < Me < *t*-Bu). This may reflect the strain relief of the substrate on going from the sp^3 to sp^2 hybridization of the 2 carbon. Rates of hydration of **2** (k_2) increase in the opposite direction (H > Me > *t*-Bu). We could not measure the rate of decay of **2a** by mixing the acetonitrile solution of **2a** with water on a stopped-flow apparatus. The rate constant k_2 for **2a** may be well greater than $100\ s^{-1}$. The value of pK_2 for **2a** may accordingly be smaller than −1.37.

The pK_R values for the equilibrium between the cation **2** and thiol ester **4** increase in the order **2c** < **2a** < **2b**. This unusual order of the pK_R may arise from the opposite influence of the 2-alkyl group on the two equilibria **2** ⇌ **3** and **3** ⇌ **4**. The unsubstituted derivative most readily cyclizes but least easily ionizes. The overall equilibrium constant is in between those for **2b** and **2c**. Difference in the alkyl groups, methyl and *tert*-butyl, influences little the magnitude of K_3 but considerably that of K_2. As a result, pK_R for **2c** is smaller than that for **2b**. Rates of both acid- and base-catalyzed decay of the tetrahedral intermediate **3** are not much dependent on the 2-alkyl group.

(30) Santry, L. J.; McClelland, R. A. *J. Am. Chem. Soc.* **1983**, *105*, 3167–3172.

Experimental Section

Materials. 1,2-Bis(1,3-dithiolan-2-ylthio)ethane (**5**) was obtained by the reaction of trimethoxymethane with 1,2-ethanedithiol catalyzed by perchloric acid.[8]

1,3-Dithiolan-2-ylium (2a) Perchlorate. To an ice-cooled solution of **5** (1.5 g) in acetic anhydride (30 mL), 70% perchloric acid (1.5 mL) was added dropwise in 15 min under stirring. The salt was precipitated by the addition of dry ether (50 mL), collected on a glass filter, washed with ether, and dried under reduced pressure to give a practically pure product: UV ($HClO_4$) λ_{max} 333 nm (ϵ 7600); NMR (CF_3CO_2D) δ 4.50 (s, 4 H), 11.35 (s, 1 H).

2-Methoxy-1,3-dithiolane (1a). The perchlorate of **2a** prepared from 1.5 g of **5** was dissolved in dry acetonitrile (30 mL), and the resulting solution was added into sodium methoxide solution (ca. 2 M) in methanol (10 mL) on an ice bath. The products were taken up with ether, washed with water, dried over $MgSO_4$, and distilled with a Kugelrohr apparatus after evaporation of the ether. The distillate (0.5 g) was collected at the oven temperature of 130 °C under 10 mmHg: [lit.[31] bp 57–61 °C (0.1 mmHg)]; NMR (CCl_4) δ 3.23 (s, 3 H), 3.1–3.3 (m, 4 H), 6.25 (s, 1 H).

2-*tert*-Butyl-1,3-dithiolan-2-ylium (2b) Perchlorate. To an ice-cooled mixture of trimethylacetyl chloride (3 mL) and 1,2-ethanedithiol (2 mL), 70% perchloric acid (2.5 mL) was added dropwise under stirring. After 10-h reaction at room temperature, acetic anhydride (15 mL) and then dry ether (50 mL) were added to the mixture on an ice bath. The precipitated yellow solid was collected on a glass filter, washed with ether, and dried in vacuo: UV ($HClO_4$) λ_{max} 331 nm (ϵ 7700); NMR (CF_3CO_2D) δ 1.68 (s, 9 H), 4.46 (s, 4 H).

2-*tert*-Butyl-2-methoxy-1,3-dithiolane (1b). The salt of **2b** prepared from 3 mL of trimethylacetyl chloride was dissolved in dry acetonitrile (30 mL). Methanol (10 mL) was added to the solution, and then triethylamine was added until the red–yellow color faded away. The products were taken up with ether, washed with water, and dried over $MgSO_4$. After the evaporation of the ether, the remaining low-melting solid was distilled: bp 110 °C (2 mmHg); NMR (CCl_4) δ 1.14 (s, 9 H), 3.2–3.3 (m, 4 H), 3.40 (s, 3 H).

(*S*)-2-Mercaptoethyl trimethylthioacetate (**4b**) was prepared by the reaction of trimethylacetyl chloride with 1,2-ethanedithiol in chloroform in the presence of pyridine:[32] bp 104–105 °C (12 mmHg); UV (H_2O) λ_{max} 233 nm (ϵ 4700); NMR (CCl_4) δ 1.20 (s, 9 H), 1.43 (t, 1 H), 2.4–3.1 (m, 4 H).

Equilibrium and Kinetic Measurements. Reactions were carried out at 25.0 ± 0.1 °C in aqueous solutions containing 1 vol % acetonitrile, the ionic strength being maintained at 0.50 M with KCl, and monitored spectrophotometrically on a Shimadzu UV 200 spectrophotometer as before.[5] Stopped-flow measurements of the rates of disappearance of **2b** were made by mixing equal volumes of the acetonitrile solution of **2b** and a dilute HCl solution (μ = 0.50 M) at 25.0 ± 0.2 °C on a Union RA 1200 apparatus.[5] The pH values of buffer solutions were measured on a Hitachi-Horiba F7 pH meter. The pD values of deuterium solutions were determined by adding 0.40 to the pH meter readings.[34] Values of the H_0 and H_R acidity functions were calculated by using the polynomial expressions supplied by Kresge et al.[10]

Registry No. 1a, 36069-31-5; **1b**, 96503-41-2; **2a**·ClO_4, 96503-38-7; **2b**·ClO_4, 96503-40-1; **1b**, 96503-42-3; **5**, 33145-02-7; $CNCH_2CO_2^-$, 23297-32-7; HCO_2^-, 71-47-6; D_2O, 7789-20-0; $ClCH_2CO_2^-$, 14526-03-5; $MeOCH_2CO_2^-$, 20758-58-1; $MeOCH_2CO_2H$, 625-45-6; $CNCH_2CO_2H$, 372-09-8; $ClCH_2CO_2H$, 79-11-8; H_2O, 7732-18-5; D_2, 7782-39-0; trimethoxymethane, 149-73-5; 1,2-ethanedithiol, 540-63-6; trimethylacetyl chloride, 3282-30-2.

Supplementary Material Available: Rate constants and equilibrium absorbances (6 pages). Ordering information is given on any current masthead page.

(31) Stüz, P. Stadler, P. A. *Helv. Chim. Acta* **1972**, *55*, 75–82.
(32) Rylander, P. N.; Tarbell, D. S. *J. Am. Chem. Soc.* **1950**, *72*, 3021–3025.
(33) Clark, W. M. "Oxidation-Reduction Potentials of Organic Systems"; Williams and Wilkins: Baltimore, 1960; pp 149–155.
(34) Bates, R. G. "Determination of pH"; Wiley: New York, 1973; pp 375–376.